

Forcing Mechanisms of Internal Rear-Flank Downdraft Momentum Surges in the 18 May 2010 Dumas, Texas Supercell

Patrick S. Skinner¹, Christopher C. Weiss², Louis J. Wicker¹, Corey K. Potvin^{1,3}, and David C. Dowell⁴

¹NOAA/National Severe Storms Laboratory, ²Texas Tech University, ³Cooperative Institute for Mesoscale Meteorological Studies/University of Oklahoma, ⁴NOAA/

Earth System Research Laboratory/Global Systems Division

Introduction

Multiple internal internal rear-flank downdraft (RFD) momentum surges were observed over a short period in the 18 May 2010 Dumas, Texas supercell sampled by VORTEX2 (Fig. 1) (Wurman et al. 2012). These surges were found to occur coincident with intensification of a low-level mesocyclone and were hypothesized to be primarily driven by perturbation pressure gradient forcing associated with the low-level mesocyclone (Skinner et al. 2014).

The origin and forcing of the internal RFD surges is further explored herein by assimilation of multiple Doppler radars into a numerical model in order to retrieve representative, three-dimensional wind and thermodynamic fields from within the Dumas supercell. These analyses allow perturbation pressure retrievals and quantitative analyses of the internal RFD surge forcing mechanisms to be undertaken.

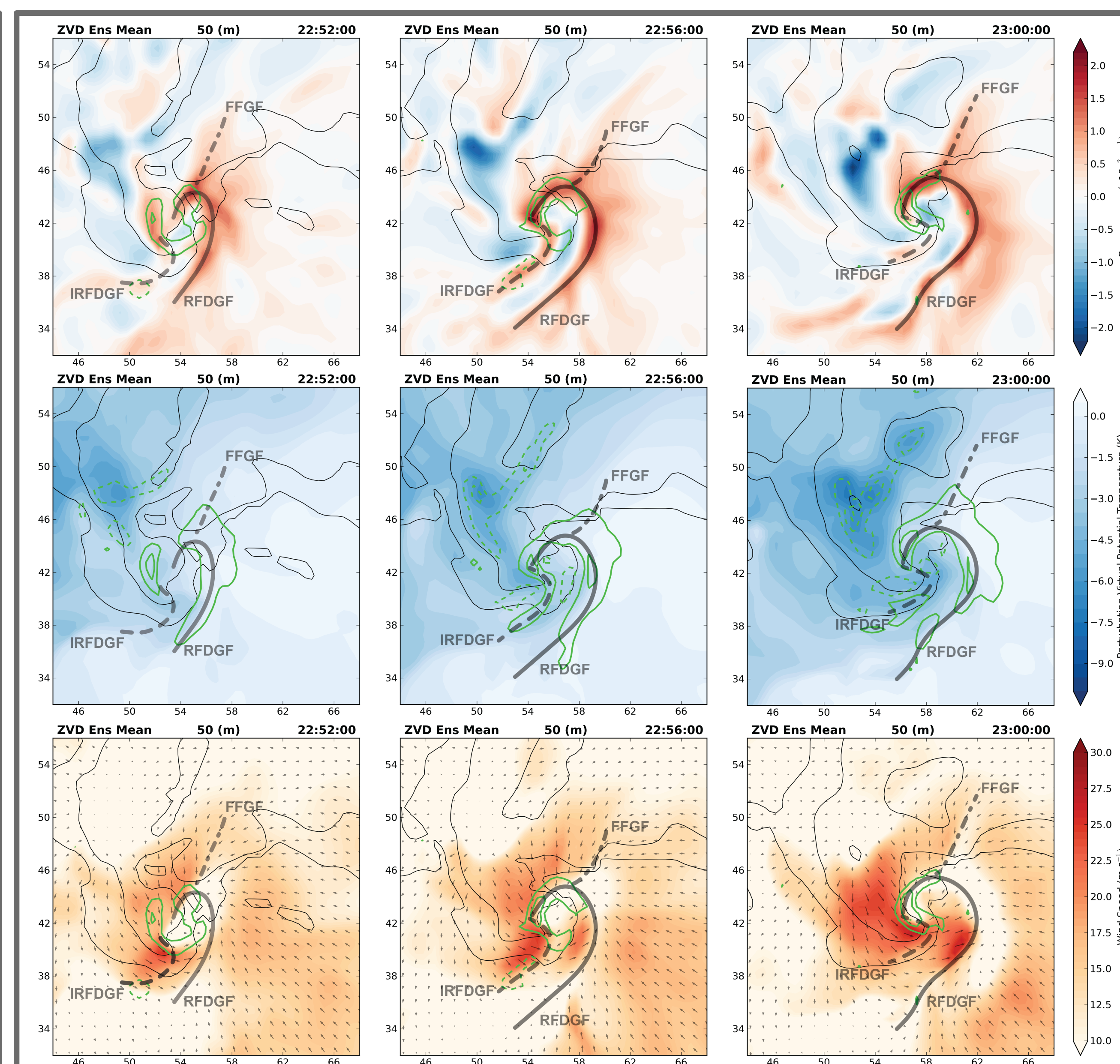


Figure 3. Ensemble mean analyses of (top row) convergence (s^{-1}), (middle row) density potential temperature (K), and (bottom row) wind speed ($m s^{-1}$) at (left column) 2252, (middle column) 2256, and (right column) 2300 UTC. The top and bottom (middle) rows contour vertical vorticity (vertical velocity) values at 500 m in green with a $0.01 s^{-1}$ ($3 m s^{-1}$) contour interval and 20 and 40 dBZ simulated reflectivity are contoured in black. Subjectively analyzed positions of the forward flank gust front (FFGF), RFD gust front (RFDGF), and internal RFD surge gust front (IRFDGF) are indicated by stippled, solid, and dashed lines, respectively.

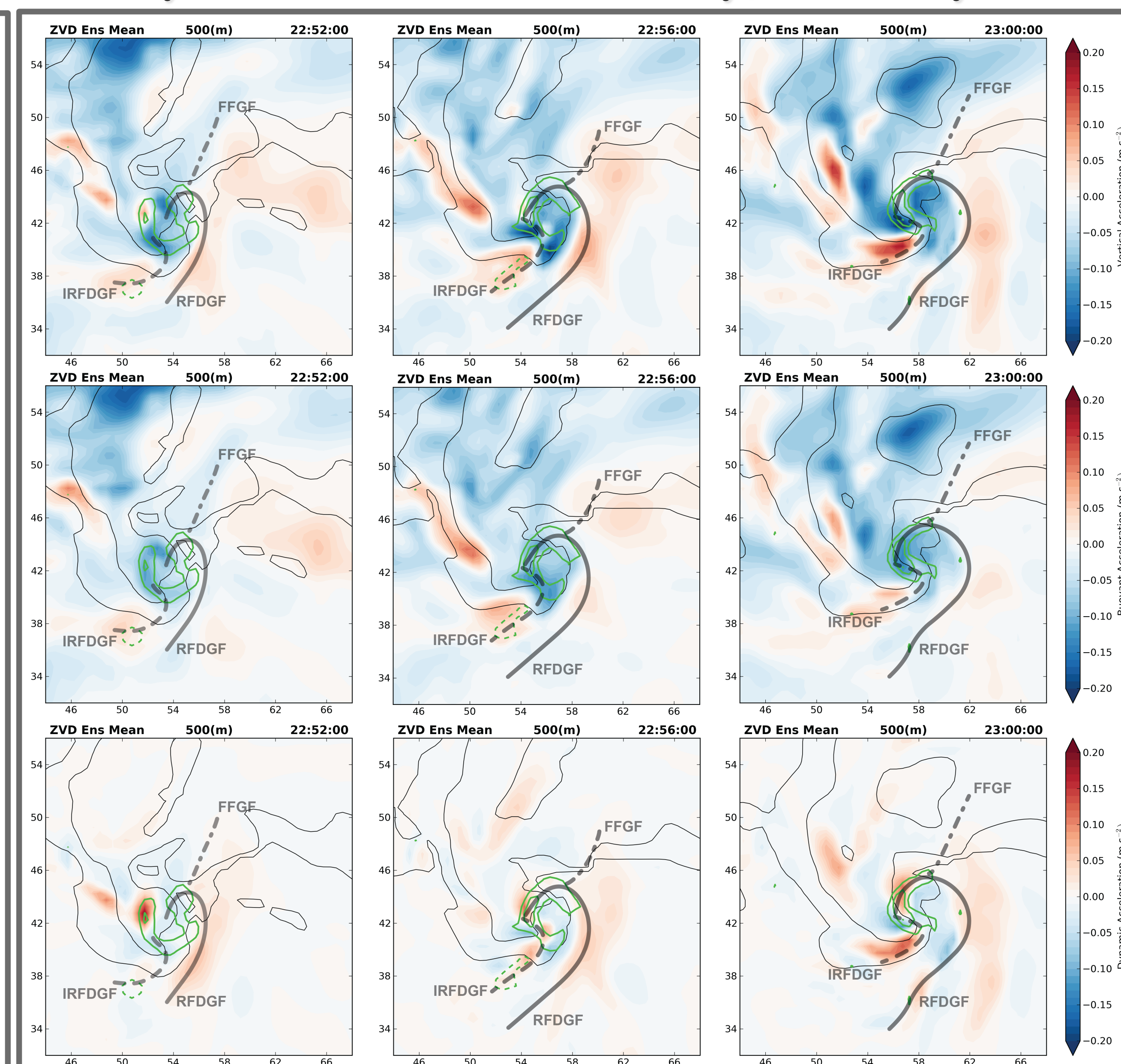


Figure 4. As in Fig. 3 except for ensemble mean components of the vertical momentum equation, (top row) total vertical acceleration ($m s^{-2}$), (middle row) buoyant acceleration ($m s^{-2}$), and (bottom row) dynamic acceleration ($m s^{-2}$). Vertical vorticity at 500 m is contoured in green for each panel and subjectively analyzed gust front position are identical to positions in Fig. 3 in order to provide a spatial reference.

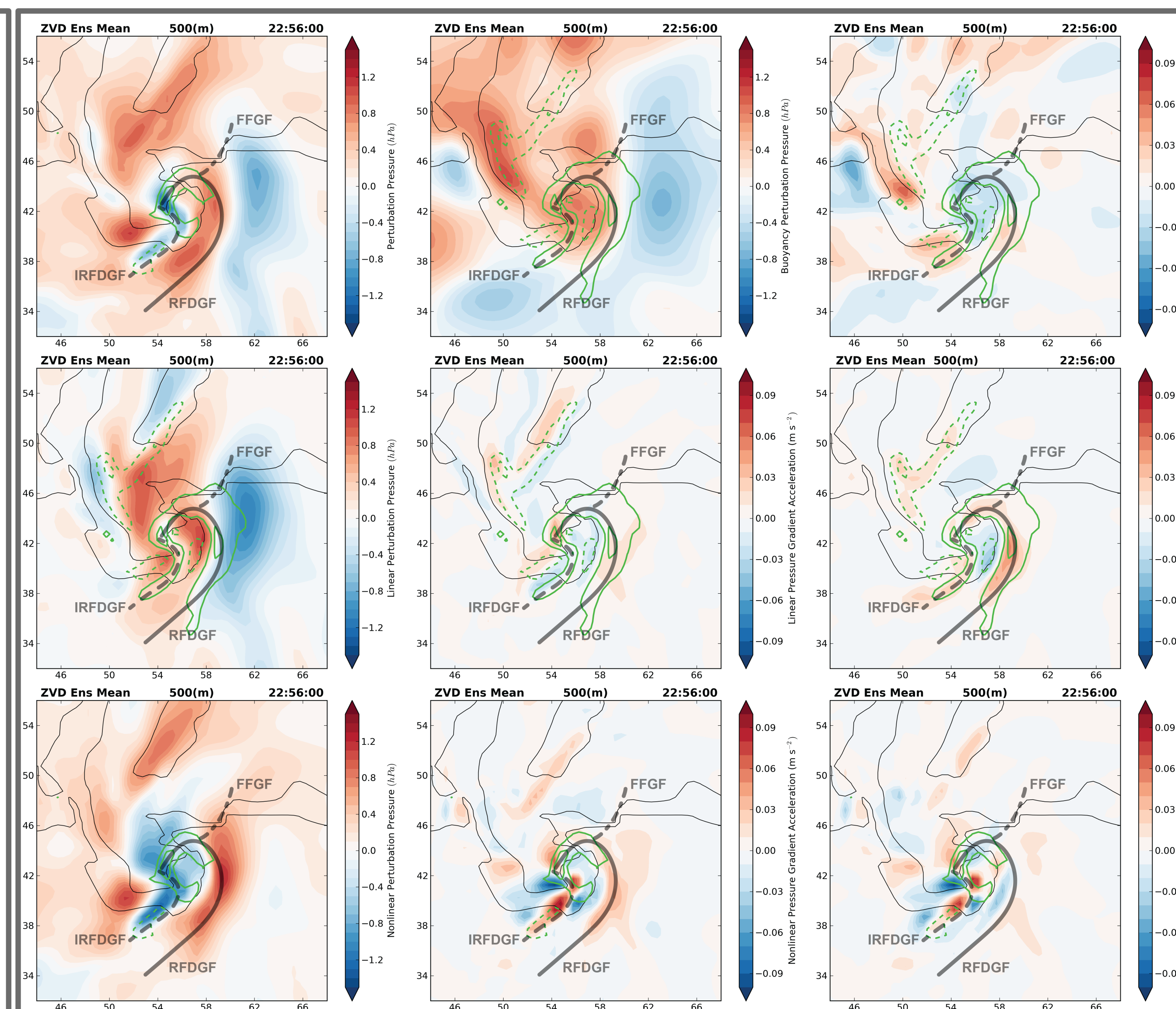


Figure 5. As in Fig. 3 except for (top left) total retrieved perturbation pressure and the (middle left) linear, (bottom left) nonlinear, (top middle) buoyant components. Vertical perturbation pressure gradient accelerations from the linear, nonlinear, buoyant, nonlinear extension, and nonlinear shear components of the perturbation pressure are plotted in the center, bottom middle, top right, middle right, and bottom right panels, respectively. Vertical velocity is contoured in green for the middle row and top right panels and vertical vorticity in the remainder of the panels.

Summary

A trough of low perturbation pressure produced primarily by the nonlinear shear terms is responsible for the development of an internal RFD momentum surge in the Dumas supercell (Fig. 5). Parcels originating near the surface in the precipitation core experience a favorable horizontal pressure gradient acceleration as the wrap around the low-level mesocyclone and approach the trough (Fig. 6). After crossing the trough axis, parcels encounter an adverse horizontal pressure gradient force, resulting in a rapid deceleration and the formation of a convergence boundary bounding a local maximum in wind speed within the broad RFD.

It is hypothesized that the development of the trough may result from occlusion of the low-level mesocyclone (Fig. 8). As the mesocyclone occludes, counter-rotating vortices will be displaced rearward from the RFD gust front, resulting in a rotationally-induced trough within the broad-scale RFD and development of an RFD surge.

Methodology

Three-dimensional wind and thermodynamic retrievals of the Dumas supercell are produced by assimilating mobile Doppler radar from the Doppler on Wheels (DOW) (Wurman et al. 1997) and Shared Mobile Atmospheric Research and Teaching Radar (SMART-R) (Biggerstaff et al. 2005) platforms, as well as WSR-88D data from KAMA (Fig. 2) into an ensemble of numerical simulations using an ensemble Kalman Filter (EnKF). A summary of model, data assimilation, and radar data objective analysis methods is provided in Table 1.

As pressure is not typically updated in Ensemble Kalman Filtering (Tong and Xue 2005), perturbation pressures are retrieved from the ensemble mean wind and thermodynamic fields. By taking the divergence of the vertical momentum equation and linearizing about the model initial state, a series of Poisson equations for the nonlinear, linear, buoyant, nonlinear shear, and nonlinear extension components of the perturbation pressure are produced (e.g. Markowski 2002). The Poisson equations are then solved following the methodology outlined in Rotunno and Klemp (1982) with Dirichlet boundary conditions enforced. Low-frequency noise in the retrievals is removed by subtracting a 21-point convolution operator from the original solution.

Parcel origins are assessed by calculating backwards trajectories for a series of 10000 – point material circuits. Trajectories are calculated using a fourth-order Runge-Kutta scheme, with linear interpolation in time between each available EnKF analysis and trilinear interpolation in space. An integration time step of 1 s is utilized and trajectories that fall below the lowest model level are calculated according to the values from the lowest grid level.

Analysis

EnKF ensemble mean analyses reproduce the observed internal RFD momentum surge and associated gust front (Fig. 3). The internal RFD surge wraps cyclonically around the low-level mesocyclone, has counterrotating vortices straddling its leading edge, and contains larger density

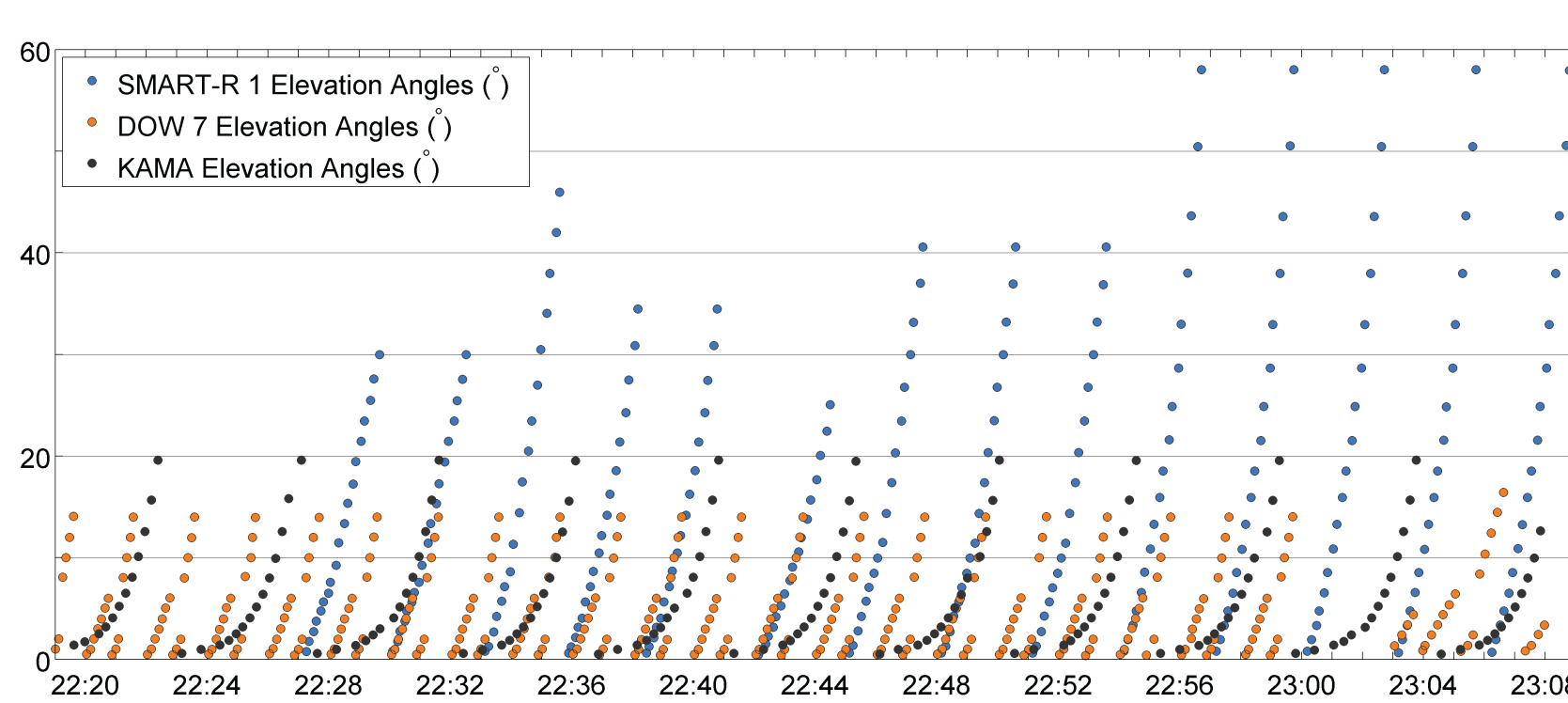


Figure 2. Time-series of SMART-R (blue), DOW (orange), and KAMA (black) elevation angles assimilated during the experiment.

Analysis Cont. – thermodynamic deficits than the broad RFD, which is similar to observations of the Dumas supercell and prior observations of internal RFD surges (e.g. Marquis et al. 2008; Lee et al. 2012; Marquis et al. 2012). Buoyant acceleration provides a strong “background” of downward acceleration across the low-level mesocyclone and RFD, with weak upward acceleration along the RFD surge gust front primarily produced by dynamic acceleration (Fig. 4). This upward acceleration is primarily produced by the nonlinear shear component of perturbation pressure and is coincident with a trough of low perturbation pressure along the gust front (Fig. 5). Material circuit analyses reveal that parcels within the RFD surge originate in the precipitation core north of the low-level mesocyclone before wrapping around the mesocyclone and accelerating due to a horizontal pressure gradient force (Fig. 6). A second parcel source region aloft does not extend below 400m (Fig. 7).

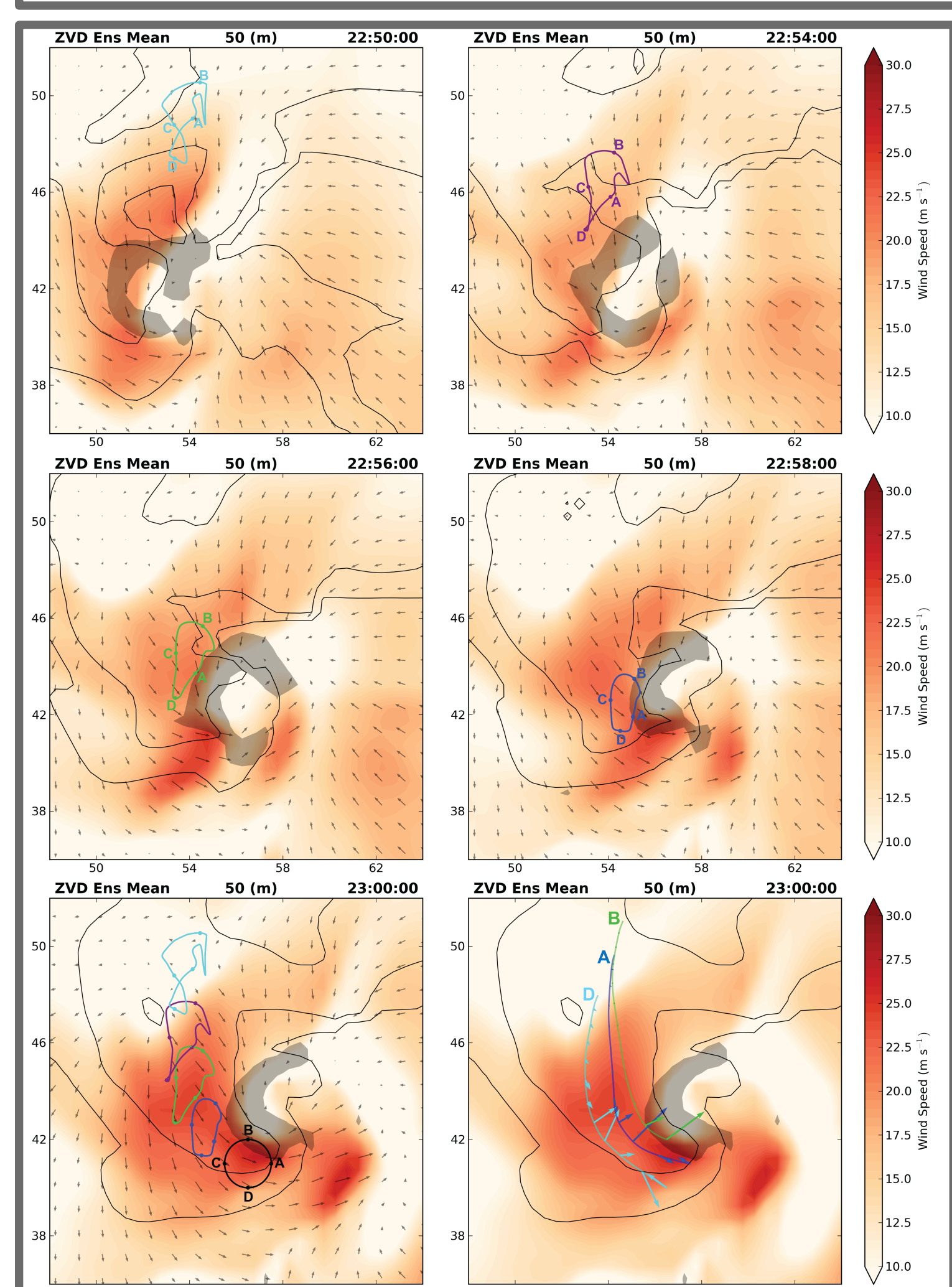


Figure 6. Ensemble mean wind speed and material circuit at (top left) 2250, (top right) 2254, (middle left) 2256, (middle right) 2258, and (bottom left) 2300. Every 2500th trajectory is marked “A” – “D” and vertical vorticity at 467 m greater than $0.01 s^{-1}$ is shaded gray. Panel at bottom right shows trajectories “A”, “B”, and “D” in blue, green, and cyan with vectors indicating horizontal perturbation pressure gradient force at 60 s increments.

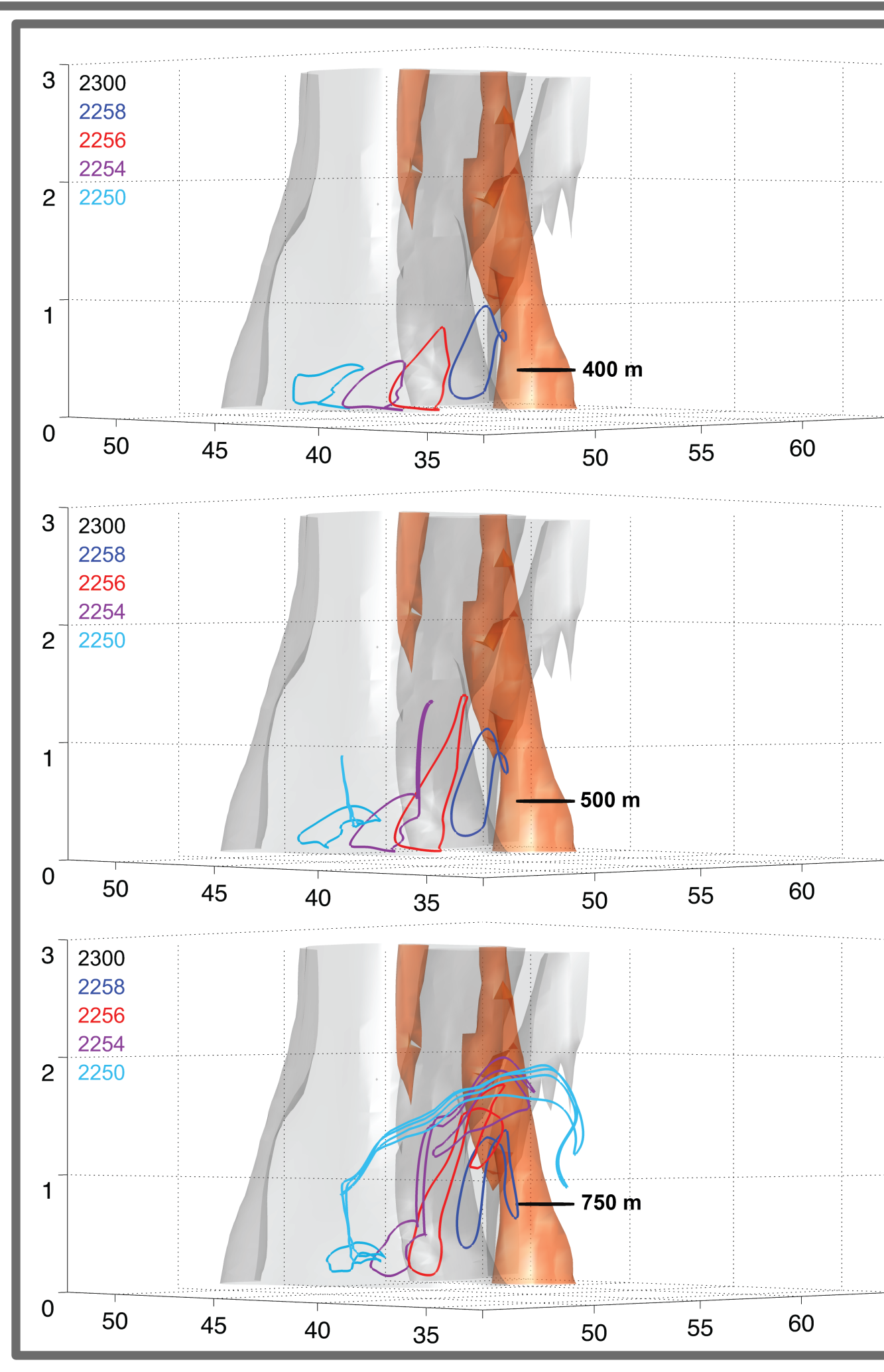


Figure 7. Color-coded locations of material circuits released at (top) 400 m, (middle) 500 m, and (bottom) 750 m. Ensemble mean isosurfaces of 40 dBZ simulated reflectivity and $0.02 s^{-1}$ vertical vorticity are plotted in gray and orange, respectively. Viewing angle is from the southwest at a 0° elevation and the vertical axis has been stretched by a factor of 4 for clarity.

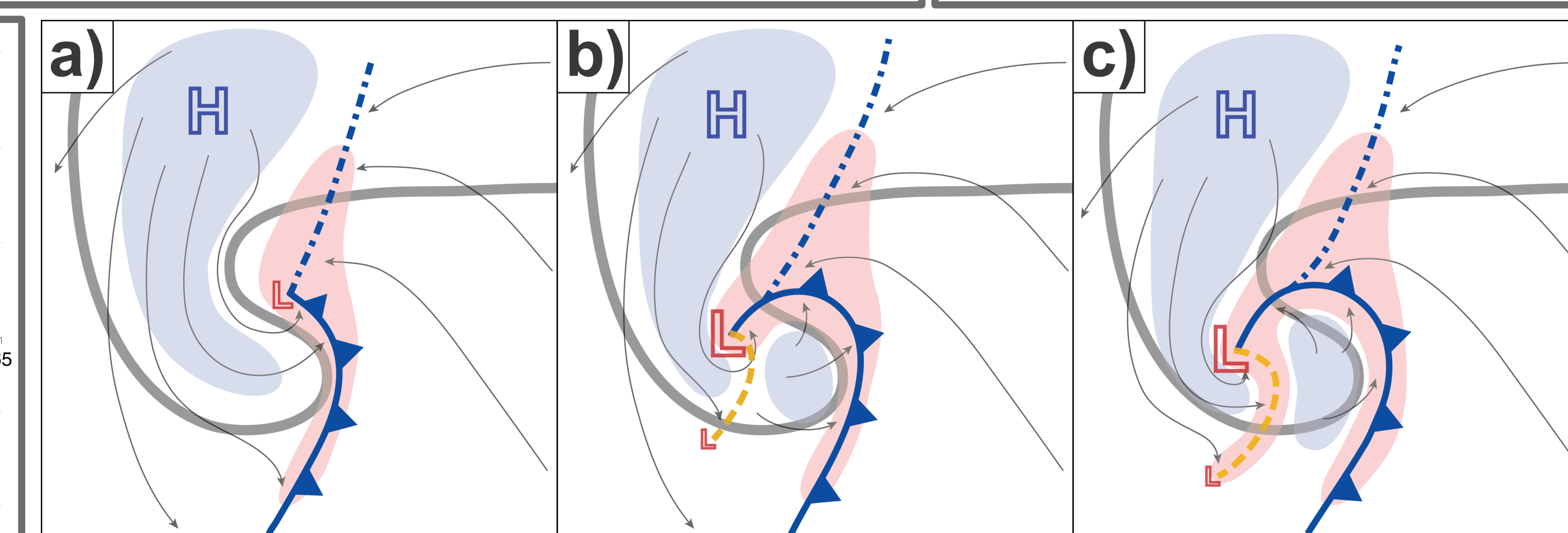


Figure 8. Proposed schematic for the near-surface formation of an internal RFD momentum surge gust front. Areas of updraft/downdraft are shaded blue/red with areas of relative low/high pressure are indicated by red “L” (blue “H”) symbols. The near-surface precipitation field is bounded by a thick, gray contour and idealized streamlines are plotted as thin, gray vectors. The cold frontal, trough, and stippled boundaries indicated the locations of the RFD gust front, internal RFD gust front, and forward flank gust front, respectively.

Acknowledgements

This research was supported by National Science Foundation Grant AGS-0964088, an NRC research associateship awarded to the first author, and the NOAA Warn on Forecast project. We wish to thank Drs. Josh Wurman, Karen Kosiba, and Michael Biggerstaff for collecting and making available DOW and SMART-R data, which were generously hosted by NCAR/EOL under sponsorship of the National Science Foundation. We are grateful for many helpful conversations with Tony Reinhart, Dr. Jim Marquis, and Dr. Dan Dawson and for the dedication of all VORTEX2 participants. References available upon request.

*Corresponding Author Address: Patrick Skinner, NOAA/SSL, 120 David L. Boren Blvd., Suite 3333 Norman, OK 72072, patrick.skinner@noaa.gov